journal

J. Am. Ceram. Soc., **82** [5] 1187–95 (1999)

Influence of Isothermal Chemical Vapor Deposition and Chemical Vapor Infiltration Conditions on the Deposition Kinetics and Structure of Boron Nitride

Marc Leparoux[†] and Lionel Vandenbulcke[*]

Laboratoire de Combustion et Systèmes Réactifs, Centre National de la Recherche Scientifique (CNRS), 45071 Orléans, France

Christian Clinard[‡]

Centre de Nanoscopie Electronique Analytique (CNEA), Faculté des Sciences, Université d'Orléans, 45067 Orléans, France

An experimental study has been performed to gain some insight into the correlations between the deposition conditions and the structure of boron nitride (BN) coatings that are used in ceramic-matrix composites. BN has been deposited at 700°C from BCl_3–NH_3–H_2 mixtures on various substrates, by using chemical vapor deposition (CVD) and isothermal–isobaric chemical vapor infiltration (ICVI) processes, simultaneously in the same reactor. A kinetic study has shown that the CVD process is governed either by a combination of mass transfer with chemical kinetics at low flow rates or by the heterogeneous kinetics only at high flow velocities. In contrast, the limiting contribution of mass transfer always is observed for the ICVI process. The influence of diffusion cages that are positioned around the fibrous preforms is reported. The structure of BN deposits has been studied as a function of the various deposition conditions via transmission electron microscopy. The chosen CVD conditions lead to a poor organization of the BN deposits. Fairly well-organized BN coatings are deposited on all fibers of a fibrous preform via ICVI. The results are discussed in terms of supersaturation and deposition yields. The use of diffusion cages and the adjustment of the inlet composition and mass flow rate seem to be very important to obtain the best BN organization and thickness uniformity.

I. Introduction

THE potential of fiber-reinforced ceramic-matrix composites (CMCs) for thermomechanical applications is well established, because of their fracture toughness, damage tolerance, and low density. The mechanical properties of CMCs are dependent largely on the fiber–matrix bonding, which must be weak enough to allow crack deflection along the interface, yet strong enough to retain load transfer from the matrix to the fibers.[1–4] A carbon-rich layer that is formed *in situ* between the fibers and the matrix during composite processing or a pyrocarbon interphase that is deposited on the fibers prior to matrix manufacturing leads to this nonbrittle mechanical behavior.[5–8] Unfortunately, the efficiency of these interphases is limited by the oxidation phenomena.[9,10]

Efforts have been made to improve the oxidation resistance of CMCs with a carbon interphase. Initially, external sealant coatings that contained silicon and/or boron were proposed.[11–13] Another approach considered a multilayered C/SiC matrix or interphase that may permit more crack deflections.[14–16] These issues are examined, together with SiC/SiBC/SiC sequenced matrices,[17] to delay the access of oxygen to the carbon interphase or the fiber/interphase interface. In other studies, the oxidation resistance of the pyrocarbon interphase itself is improved by some change of its composition, as in boron-doped pyrocarbon[18] or in a compositional gradient layer, the composition of which varies continuously from the fiber interface (carbon) to the matrix interface (SiC).[19]

On the other hand, boron nitride (BN) has been proposed as an alternative, because of its graphitelike structure and its better resistance to oxidation.[20] It has been successfully used in various composite systems.[21–29] Particular attention has been given to the interfacial zones, in terms of chemistry and microstructure.[26–29] These studies revealed that many interfacial carbon- and/or SiO_2-rich sublayers can be present between the SiC fibers (Nicalon™ (Nippon Carbon, Tokyo, Japan) or Tyranno™ (UBE Industries, Yamaguchi, Japan)) and the BN film. To improve the mechanical properties, especially at high temperature, it is fundamental either to protect the carbon-rich sublayers from the external atmosphere or, even better, to prevent their development. This condition implies the formation of strong interfacial bonding and the optimization of the BN organization to deflect the cracks inside the interphase. Such an optimized structure can be examined by controlling the classical experimental deposition parameters. Together with the process type (either chemical vapor deposition (CVD) in a hot-wall reactor or isothermal–isobaric chemical vapor infiltration (ICVI)), these variables produce different deposition conditions at the gas-phase/substrate interface, which also are a function, in any case, of the total amount of fibers to be coated. Moreover, adequate deposition conditions can prevent the development of amorphous glassy sublayers as SiO_2. In previous studies,[26–29] the interfaces have been principally observed and, generally, the evolution of the structure in the BN deposit has not been described, especially as a function of the deposition conditions.

In this paper, the BN deposition was performed at 700°C from the BCl_3–NH_3–H_2 gas mixture, which was shown to be less aggressive than the BF_3–NH_3 precursor under the infiltra-

R. Naslain—contributing editor

Manuscript No. 191278. Received January 14, 1997; approved September 21, 1998.

Supported by the Société Européenne de Propulsion (SEP) and Région Centre, via a grant given to author ML.

[*]Member, American Ceramic Society.

[†]Present address: Fraunhofer–IWS, Winterbergstraße 28, 01277 Dresden, Germany.

[‡]Present address: CNRS–CRMD, 1B Rue de la Férollerie, 45071 Orléans, France.

tion conditions.[30] To gain some insight into the correlations between the deposition conditions and the BN structure, first, deposition conditions where the CVD process is purely controlled by the surface kinetics have been determined.[30,31] These conditions allow investigation of the influence of the different inlet gaseous species on the surface kinetics. Then, how the deposition conditions are influenced by mass transfer and depart from this limiting case of pure kinetic control, as a function of either the process type (CVD or ICVI), processing parameters, inlet gas composition, and/or total gas flow rate, is given in this study. The influence of diffusion cages that are positioned around the fibrous preform also is reported. Finally, the BN structure is studied, using transmission electron microscopy (TEM), under these various CVD and ICVI conditions, and the variations of the uniformity of the deposit are reported.

II. Experimental Procedure

(1) Materials and Deposition Procedure

BN was deposited by using different isothermal CVD processes at a temperature (T) of 700°C, under a reduced pressure (P) of 1.3 kPa, from BCl_3–NH_3–H_2 gas mixtures of different inlet composition. The deposition apparatus and procedure have been described in detail previously.[30–32] Considering the poor stability of BN that was obtained at the given temperature, the deposits were always thermally treated at 1000°C at the end of the deposition stage, directly in the reactor, for 2 h under vacuum (residual pressure of 1 Pa).

BN deposition was performed simultaneously on bulk substrates and a fibrous preform, to investigate both CVD and ICVI, respectively (Fig. 1). One bulk substrate was composed of ten graphite rings that were mounted on a holder. The deposition process also was applied to one-dimensional (1D) fiber substrates, which consisted of either small tows or monofilaments that were mounted on a carbon fixture, and to two-dimensional (2D) single-plane-weave fabrics. In any case, the main surface of the substrate was parallel to the gaseous flow.

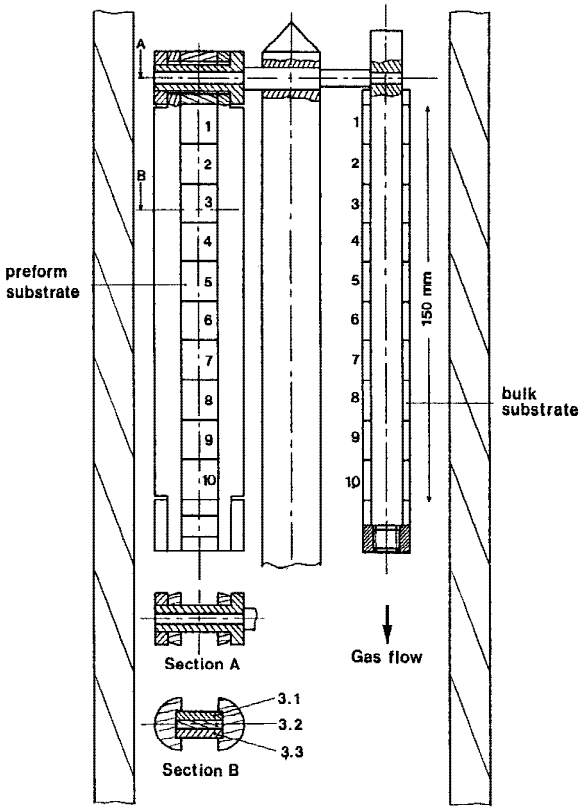

Fig. 1. Schematic of the bulk substrates and the fibrous preform with their holders in the deposition reactor.

The thickness of these fibrous substrates was always very low (<0.4 mm); therefore, the deposition conditions that have been considered in this paper were the same as (for monofilaments) or similar to (for tows) those from the CVD process. Different fibers have been used to observe the influence of the nature of the substrate: these fiber types include T300 (ex-PAN, average diameter of 8 μm; Torayca, produced by Soficar, Abidos, France) and P55 (pitch-derived, average diameter of 10 μm; Thornel, produced by Amoco Polymers, Chicago, IL) carbon fiber, as well as Nicalon™ NLM 202 fiber (ex-PCS, average diameter of 15 μm).

The infiltration process (ICVI) was investigated by using a three-dimensional (3D) woven architecture (Novoltex™, Société Européenne de Propulsion (SEP), Saint-Medard-en-Jalles, France) that was composed of carbon fibers that were 9 μm in diameter (ex-PAN, treated by SEP); this Novoltex™ material had an average pore diameter of 45 μm and a specific surface area of ~0.25 m^2/g. The fibrous preform (150 mm × 18 mm × 10 mm) was cut into thirty intermediate samples, each measuring 15 mm × 18 mm × 3.3 mm. Each element was referenced by using the nomenclature "*m.n*," where $m = 1$–10 for the longitudinal position and $n = 1$–3 for the transverse position (see Fig. 1). Thus, different parameters have been introduced to characterize the uniformity of the deposit. For the fibrous preforms, the variable LU represents the longitudinal thickness uniformity, which is calculated as the ratio between the lowest and the highest relative mass increases along the preform ($m = 1$–10). The variable IU represents the infiltration uniformity, which is defined as the average of ten ratios between the internal elemental relative mass gain ($n = 2$) and the average external mass (calculated from values for $n = 1$ and $n = 3$). The total uniformity (TU) is defined as TU = LU × IU. For the bulk substrates, the variable U represents the longitudinal uniformity, which is calculated as the ratio between the relative weight increase at the bottom and top of the ten graphite rings after smoothing the curve that reports the relative weight gain of the ten substrates.

In some cases, diffusion screens were placed in front of the fiber substrates (they were not used to protect the graphite rings). These screens created a pure diffusive volume around the substrates, which were separated from the convective flow. In case of the CVD process on monofilaments or small tows, the screens were made of carbon sheets with many holes bored into them. The screens were mounted on both sides of the fiber fixture, using a carbon-based cement. In case of ICVI, the diffusion screens were composed of graphite plates that completely surrounded the preform (Fig. 2). The gaseous phase could only diffuse through oblong holes that had been bored into the plates that were positioned in front of the main surface of the substrate. The axis of these holes was perpendicular to the external convective-flow direction, and their diameter was four times smaller than the thickness of the plate. In the following text, the terms "protected-CVD" and "protected-ICVI" are used to respectively denote CVD and ICVI processes that were performed with protection screens.

(2) Structural Characterization

The BN-coated fibers were characterized via TEM. The analyses were performed at CNEA (Université d'Orléans) on thin foils that had been prepared in a conventional manner, by inclusion in a methylmethacrylate resin or in Araldit® (Ciba Specialty Chemicals Holding, Basel, Switzerland) and cutting normal to the fiber axis via ultramicrotomy. Transverse variations of the BN structure were obtained by scanning different zones of the coating, from the interface at the fiber to the external portion of the BN deposit. Generally, three sections were observed and one representative BN coating was chosen to be studied on each specimen. The dimensions of the greatest coherent domain and the interlayer distance, which is normally 0.333 nm for hexagonal BN, were measured on the TEM images. In the reported results, L_a represents the dimension of the in-plane extension and L_c represents the extension of the co-

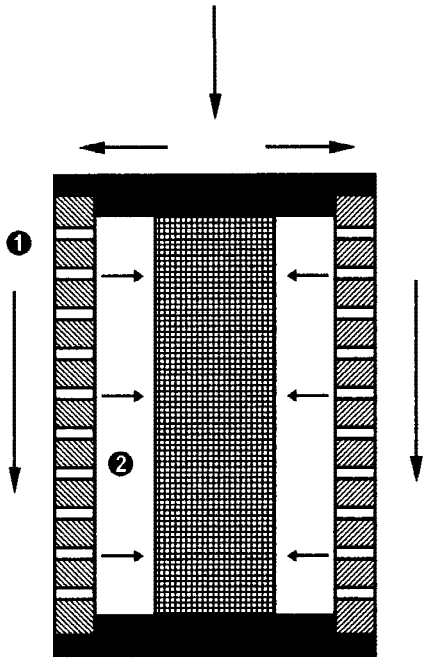

Fig. 2. Schematic of the diffusion cages with external convective flow (denoted as "1") and pure diffusion (denoted as "2") to the fibrous preform.

herent domain along the ***c***-axis of hexagonal BN. The greatest coherent domain is the domain with the greatest surface (the area is defined as $L_a \times L_c$). For the interlayer distance, a minimum of five measurements was made on each image. The average between the lowest and the greatest interlayer value is depicted in the figures, as well as the dispersion. Well-crystallized graphite was used as a standard, to measure the interlayer distance. The maximal error, from the procedures that have been used for our data acquisition, image treatments, and final measurements, was ~0.03 nm.

III. Results

(1) Deposition Kinetics

The influence of the deposition temperature on the deposition rate in the internal and external portions of the preform (ICVI) and on the graphite rings (CVD) already has been reported for equal partial pressures of BCl_3, NH_3, and H_2 and a total mass flow rate of 7×10^{-6} kg/s.[30,31] The deposition rates in the preform are dependent exponentially on the inverse of temperature in the 500°–700°C range. At higher temperatures, they stabilize and even decrease in the internal portion, thus indicating a mass-transfer limitation, which leads to poor infiltration uniformity (IU = 65% and LU = 45% at 800°C, instead of 80% and 70%, respectively, at 700°C). Such a mass-transfer limitation was not observed in CVD. However, the following study was performed at 700°C to preserve fairly good deposit uniformities via ICVI.

The influence of the mass-flow-rate variations on the CVD deposition rate on the graphite rings shows a transition in the process from a mass-transfer and chemical-kinetics control to a pure chemical kinetic limitation (Fig. 3). At flow rates greater than ~25×10^{-6} kg/s, the main control by the heterogeneous kinetics at the surface of the bulk substrates is shown either by the negligible influence of the total flow rate or by the very high value (98%) of the longitudinal uniformity (Fig. 4). The protected-ICVI process seems to be always governed by a combination of mass transfer and chemical kinetics, because of the high specific surface area of the preform, which adsorbs a large amount of reactants (Fig. 3). A slightly lower growth rate and

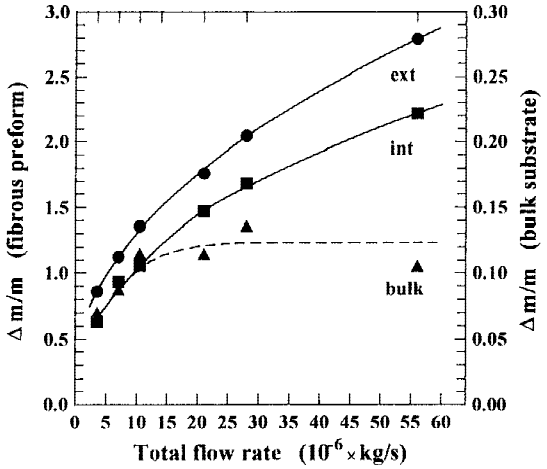

Fig. 3. Influence of the total mass flow rate on the relative weight of deposit ($\Delta m/m$) on the bulk substrate via CVD and in the internal and external portions of the fibrous preform via protected-ICVI (T = 700°C, P = 1.33 kPa, NH_3/BCl_3 = 1, and H_2/BCl_3 = 1).

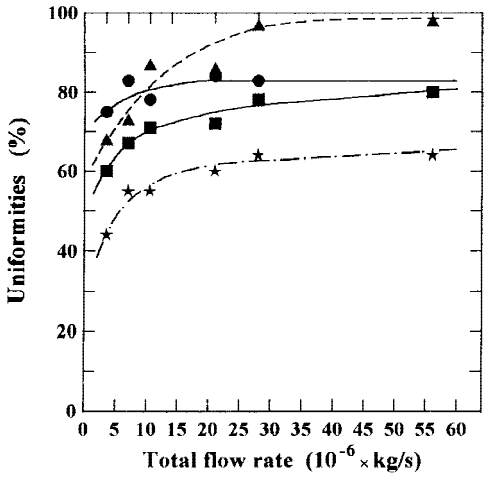

Fig. 4. Variation of the uniformities with the total mass flow rate on (▲) the bulk substrate U and in the preforms (■) LU, (●) IU, and (★) TU for protected-ICVI.

especially slightly greater uniformities are obtained by using the protected-ICVI process, in comparison to classical ICVI (see Figs. 4 and 5).

High flow rates lead to deposition conditions where the CVD process is only controlled by the surface kinetics; thus, the CVD deposition mechanism can be studied and the deposition conditions in the ICVI process can be compared. The nil order, with respect to argon, allows both the total flow rate and the total pressure to be maintained constant while the partial pressure of a species was changed, to determine the apparent reaction order with respect to this species.[30] Under these conditions, the residence time of the gaseous phase within the reactor was maintained constant. That point could be important if some homogeneous intermediate reaction occurs. On the other hand, a constant total pressure allows restriction of the variations of the diffusion conditions to the compositional effect.

The apparent reaction order, with respect to the gaseous product HCl, was observed to be zero.[30,31] Moreover, HCl has a weak influence on the BN deposition rate in the preform; this result is certainly due to similar mass-transfer conditions of the reactant species (the diffusion coefficient of argon and HCl are not very different). The experimental results that concern the reactants NH_3 and BCl_3 permit the determination of two distinct domains in either case, as shown, for example, in Fig. 6,

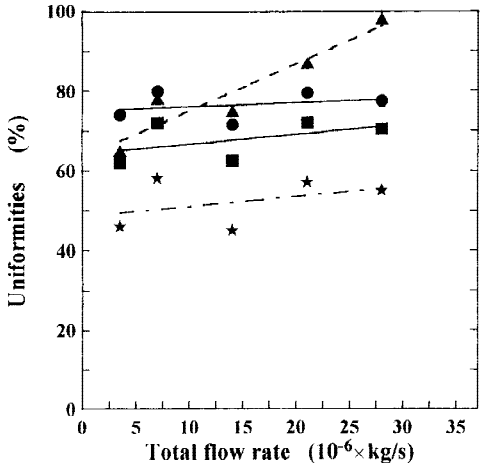

Fig. 5. Variation of the uniformities with the total mass flow rate on (▲) the bulk substrate U and in the preforms (■) LU, (●) IU, and (★) TU for classical ICVI.

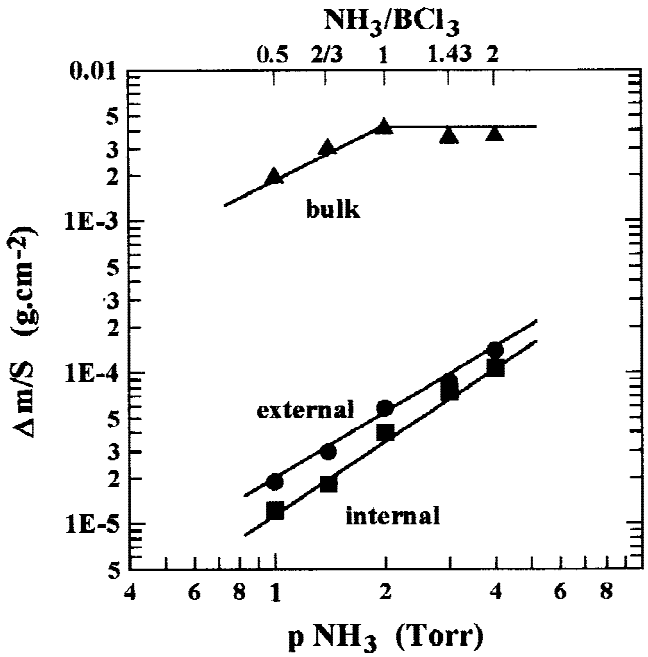

Fig. 6. Influence of the inlet partial pressure of NH_3 on the weight of deposit per surface unit ($\Delta m/S$) on the bulk substrate and in the internal and external portions of the fibrous preform for protected-ICVI (T = 700°C, P = 1.06 kPa, $p_{BCl_3} = p_{H_2}$ = 0.266 kPa (2 torr), and $f \geq 28 \times 10^{-6}$ kg/s).

where the deposition rates per surface unit are reported as a function of the inlet NH_3 partial pressure (p_{NH_3}). Similar results have been obtained with respect to BCl_3.[30] The apparent reaction orders are almost one for the minor reactant species and zero for the major reactant species that seems to be preferentially adsorbed. These results agree with a previous study that showed a first-order dependence on the BCl_3 partial pressure (p_{BCl_3}) and a nil order, with respect to NH_3, when BCl_3 was the minor reactant.[33]

In regard to the classical-ICVI or protected-ICVI processes, the deposition kinetic behaviors are different from the CVD behavior, as a function of the reactant partial pressures. Clearly, the external and internal ICVI rates continuously increase as the NH_3/BCl_3 ratio increases, as shown here for protected-ICVI (Fig. 6); however, these values remain much lower than the CVD rate. The ICVI process is not purely chemical-rate-limited, and a combination with mass transfer should be considered. Optimal infiltration rates and uniformities are attained for $p_{NH_3} > p_{BCl_3}$ (Fig. 7) but also when p_{BCl_3} increases.[30] However, these conditions could become detrimental to the molecular diffusion inside the preform if the total pressure increases too much. Moreover, some homogeneous nucleation also could occur.

Finally, these different behaviors of the CVD and ICVI processes may have an important role in the growth mechanism and the deposit structure. Results on the variations of the structure with the deposition conditions are reported in the next section.

(2) Deposit Structure

Regardless of the deposition conditions, BN presents a turbostratic structure with layers that have a tendency to lie parallel to the fiber, particularly near the fiber/BN interface. No noticeable influence of the fiber type (T300, P55, or Nicalon™) has been observed on the organization and orientation of the BN structure, especially near the fiber surface.

The influence of the local deposition conditions on the deposit structure, with respect to the process type (CVD or ICVI), was studied under the following standard conditions: T = 700°C, P = 1.33 kPa, NH_3/BCl_3 = 1, H_2/BCl_3 = 1, and a total flow rate (f) of 7×10^{-6} kg/s. The samples were taken from the middle of T300 tows and Novoltex™ preforms (these samples are referenced as "6.2") for the CVD and ICVI processes, respectively. Figure 8 presents the variations of the greatest coherent domain and the variations of the interlayer distance in the BN coating, both as a function of the distance from the fiber, for the different deposition processes. In both cases, the BN layers have a tendency to lie parallel to the fiber surface, especially near the fiber/BN interface;[30] however, no preferential growth appears that would have produced a planar ($L_c < L_a$) or columnar ($L_c > L_a$) structure. The two CVD processes—protected or not—produced similar BN film microtextures. The coherent domains were very small, except in the most-external portion (which is ~10–20 nm thick). The interlayer distances and the dispersion of the values clearly increased when the coherent domains were smaller, in the central portion of the BN deposit. The ICVI processes allowed deposition of BN coatings that globally exhibited better organization with greater coherent domains and smaller interlayer distances. These two parameters also were clearly correlated for

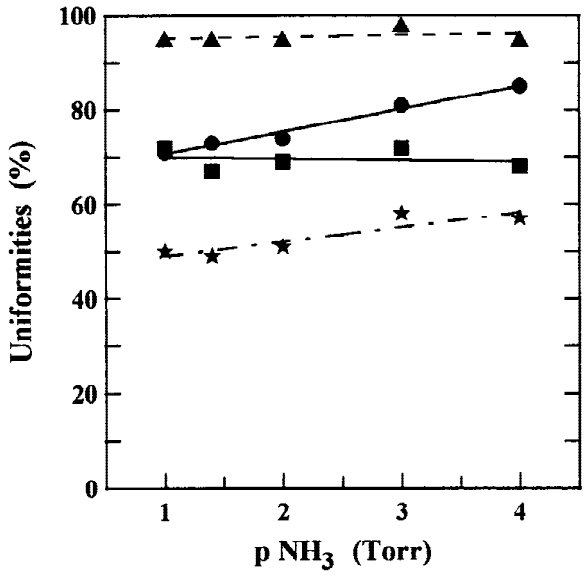

Fig. 7. Variation of the uniformities with the inlet partial pressure of NH_3 on (▲) the bulk substrate U and in the preforms (■) LU, (●) IU, and (★) TU for protected-ICVI (T = 700°C, P = 1.06 kPa, $p_{BCl_3} = p_{H_2}$ = 0.266 kPa (2 torr), and $f \geq 28 \times 10^{-6}$ kg/s).

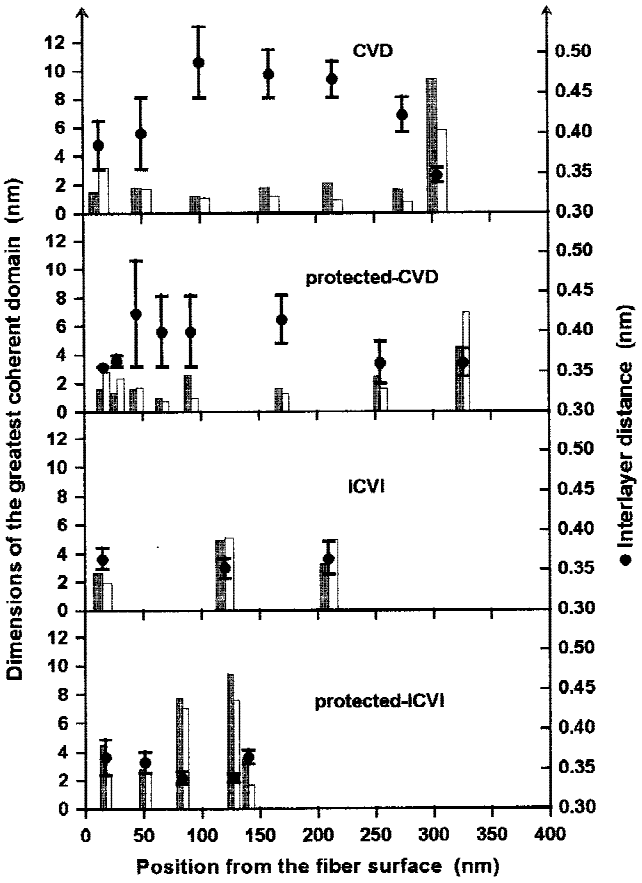

Fig. 8. Evolution of the greatest coherent domain and the interlayer distance in the BN thickness for different processes. Samples were taken in the middle of the tows or of the fibrous preforms (the 6.2 specimen reference). L_c and L_a data are shaded gray and white, respectively (T = 700°C, P = 1.33 kPa, NH_3/BCl_3 = 1, H_2/BCl_3 = 1, and $f = 7 \times 10^{-6}$ kg/s).

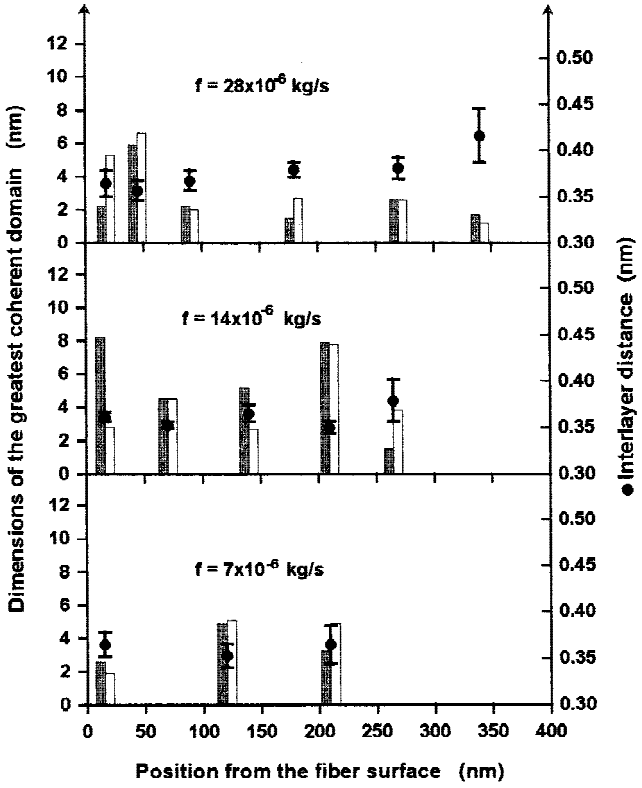

Fig. 9. Evolution of the greatest coherent domain and the interlayer distance in the BN thickness, as a function of the mass flow rate for the classical ICVI process. L_c and L_a are shaded gray and white, respectively. Samples were taken in the middle of the fibrous preforms (the 6.2 specimen reference).

the ICVI processes. No "skin effect" was observed in the most-external portion, in contrast to the CVD coatings. The range of the interlayer distances was narrow, and values as low as 0.33 nm (which corresponds to the theoretical distance for a hexagonal BN crystal) were observed. The protected-ICVI process produced the best organization, with lower standard deviations of the interlayer spacing.

The evolution of the structure of the deposits in the middle of the Novoltex™ preform has been observed for three total flow rates—7×10^{-6}, 14×10^{-6}, and 28×10^{-6} kg/s—for both ICVI processes. Figure 9 shows the variation of the greatest coherent domain and the interlayer distance from the carbon-fiber/BN interface to the external portion of a coating that has been deposited via classical ICVI. The two lowest mass flow rates lead to similar structures; however, the BN organization seems to be slightly better at a flow rate of 14×10^{-6} kg/s. In contrast, the BN organization is altered for the highest flow (i.e., at 28×10^{-6} kg/s), especially at distances greater than ~50 nm from the fiber surface. Figures 10(a) and (b) respectively illustrate the structures that have been obtained for this flow rate at a distance of ~50 nm from the fiber and near the fiber/BN interface. Figure 10(a) is representative of one of the poorest BN lattice organizations. However, this organization presents characteristics that are even better than the structure that is generally observed in the CVD coatings, except in their external portion. In contrast, with the protected-ICVI process, this relatively high flow rate produces the best BN organization, as shown in the micrographs in Fig. 11. Figure 12 confirms the large dimensions of the greatest coherent domain. The crystal growth seems to be preferentially columnar, i.e., $L_c > L_a$. In any case, the interlayer distances remain relatively small, with average values of ~0.35 nm, all along the BN film (Fig. 12). An additional experiment that was conducted at a flow rate of 56×10^{-6} kg/s led to a BN structure that was similar to that obtained at a flow rate of 14×10^{-6} kg/s.

At each position of the substrate to be coated, the deposition and growth conditions obviously are dependent on the partial pressures of all the species that are present. Therefore, the structure of the BN coating that has been deposited using the standard conditions has been investigated for three different positions in the fibrous preform. For example, Fig. 13 shows results that have been obtained with the protected-ICVI process. For this fairly low mass flow rate, the results that have been obtained with classical ICVI are not very different. In any case, the 6.1 (6.3) specimen presents the best organization, as indicated by its greater coherent domains. However, all the variations that can be noted are moderate in comparison to the variations of the structure that has been produced by using the other experimental parameters. This observation is confirmed by the examination of the variations of the interlayer distances. The interlayer distances remain relatively small and are only slightly dispersed, regardless of the position and the infiltration process.

A particular skin effect was observed for the CVD processes (Fig. 8). Observation of the microtexture with and without the thermal post-treatment clearly shows that this effect results from the post-treatment. For ICVI processes, such an effect never appeared. In addition to the standard treatment, different treatment times were tested at 1000°C (1 and 4 h) and a treatment at 1200°C was performed for 2 h. Moreover, other treatments were conducted at 1.33 kPa in various gaseous atmospheres, which included hydrogen, argon, nitrogen, and helium. Unfortunately, no improvement of the BN lattice organization was observed. An alternate CVD process that involved several short deposition steps, using standard condi-

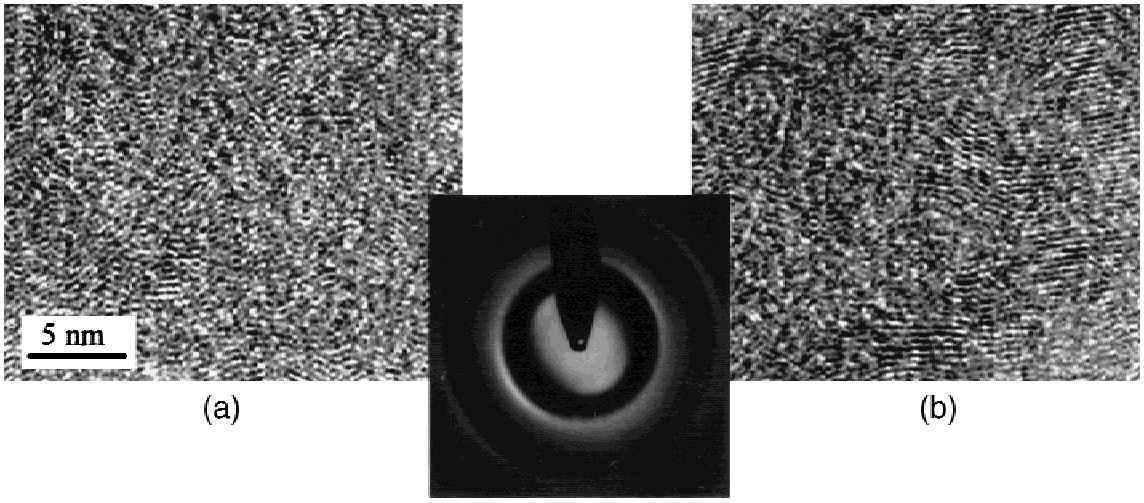

Fig. 10. TEM lattice fringes of the BN coating obtained by classical ICVI ($f = 28 \times 10^{-6}$ kg/s) ((a) inside the BN deposit and (b) near the fiber/BN interface); the electron-diffraction result also is shown.

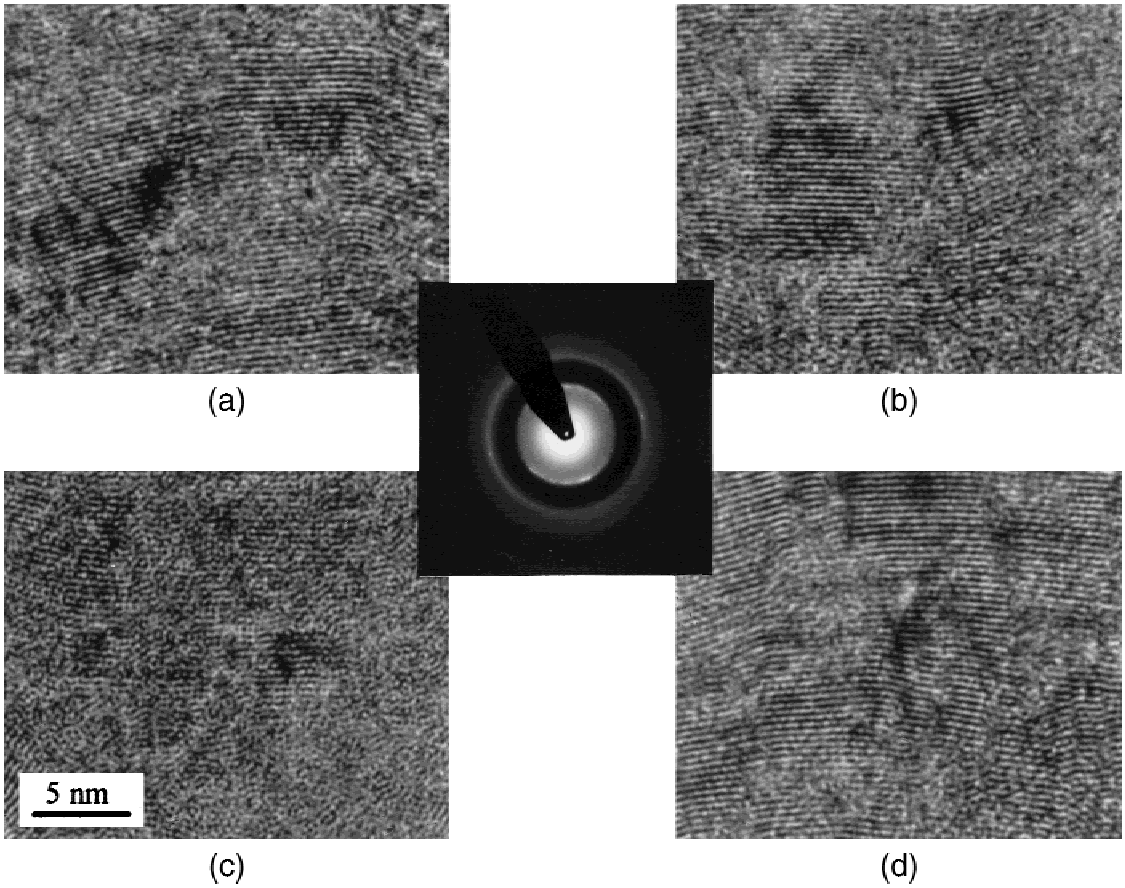

Fig. 11. TEM lattice fringes of the BN coating obtained via protected-ICVI ($f = 28 \times 10^{-6}$ kg/s) ((a) the external portion of the deposit, (b) between the external portion and the middle, (c) the middle of the coating, and (d) near the fiber/BN interface); the electron-diffraction result also is shown.

tions, followed by thermal treatment steps did not permit either process to improve the BN organization.

IV. Discussion

At 700°C, the CVD process is limited either by a combination of mass transfer with the chemical kinetics at low flow rates or by the chemical kinetics alone at high flow rates where the deposition rate is only governed by the partial pressure of the reactant (p_{BCl_3} or p_{NH_3}, whichever has the lowest value). In all cases, the deposition conditions at the gas/solid interface depart very much from the approximate equilibrium between the gas phase and the solid; i.e., the supersaturation is high. If we suppose that no intermediate precursors are produced via homogeneous reactions, a local equilibrium at the interface would be represented by reaction (1):

$$BCl_3 + NH_3 \rightleftarrows <BN> + 3HCl \quad (1)$$

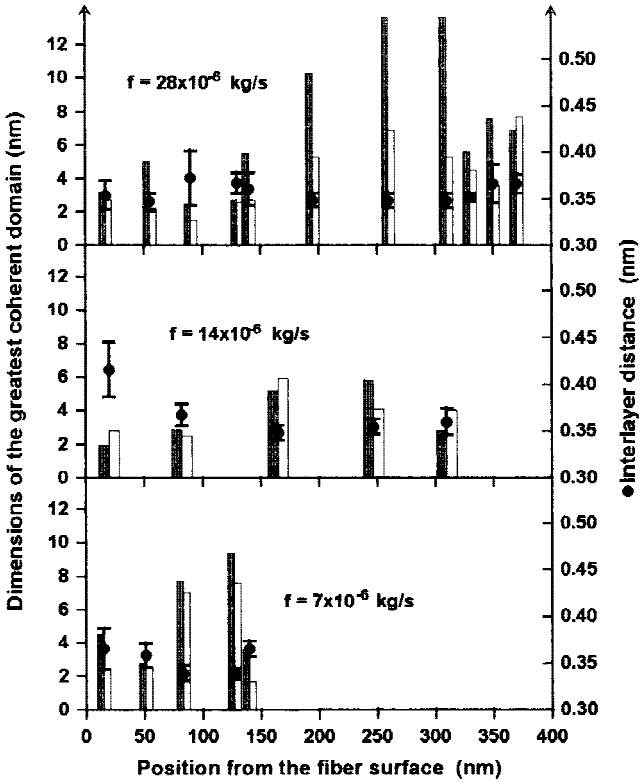

Fig. 12. Evolution of the greatest coherent domain and the interlayer distance in the BN thickness, as a function of the mass flow rate for the protected-ICVI process. L_c and L_a are shaded gray and white, respectively. Samples were taken in the middle of the fibrous preforms (the 6.2 specimen reference).

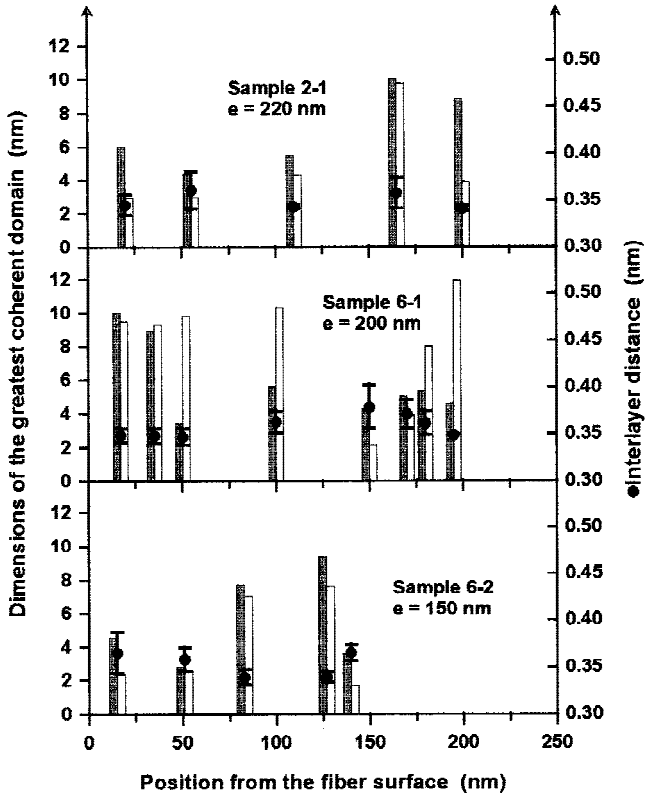

Fig. 13. Evolution of the greatest coherent domain and the interlayer distance in the BN thickness, as a function of the location in the preform for the protected-ICVI process. L_c and L_a are shaded gray and white, respectively (T = 700°C, P = 1.33 kPa, NH_3/BCl_3 = 1, H_2/BCl_3 = 1, and $f = 7 \times 10^{-6}$ kg/s).

with

$$K_p = \frac{(p_{HCl}^{eq})^3}{p_{BCl_3}^{eq} p_{NH_3}^{eq}} \tag{2}$$

Total supersaturation of the gas phase at the gas/solid interface could be defined, as a function of the actual local partial pressures in the gaseous reactants and product, by using the relation[34]

$$\Sigma_t = \frac{p_{BCl_3} p_{NH_3} (p_{HCl}^{eq})^3}{(p_{HCl})^3 p_{BCl_3}^{eq} p_{NH_3}^{eq}} \tag{3}$$

Thermodynamic calculations showed that the yield of reaction (1) was always very high at 700°C (>99%, with respect to the reactant BCl_3 or NH_3, whichever had the lowest partial pressure).[30] Therefore, one also could say that the departure from equilibrium or supersaturation is high (or low) and that the degree of completion of the reactants conversion is high (or low). In the same manner, supersaturation with respect to the elements of the BN solid can be defined if we assume a local equilibrium state in the supersaturated gas phase at the gas/solid interface, which allows determination of the actual boron and nitrogen partial pressures:

$$BCl_3 + \tfrac{3}{2} H_2 \rightleftarrows B + 3HCl \tag{4}$$

with

$$p_B = \frac{K_p' p_{BCl_3} (p_{H_2})^{3/2}}{(p_{HCl})^3} \tag{5}$$

and

$$NH_3 \rightleftarrows N + \tfrac{3}{2} H_2 \tag{6}$$

with

$$p_N = \frac{K_p'' p_{NH_3}}{(p_{H_2})^{3/2}} \tag{7}$$

The supersaturation in boron (Σ_B) and nitrogen (Σ_N) can be obtained when the actual partial pressures are compared to the boron and nitrogen partial pressures that are in equilibrium with solid BN at a given temperature (p_B° and p_N°):

$$\Sigma_B = \frac{p_B}{p_B^\circ} = \frac{K_B p_{BCl_3} (p_{H_2})^{3/2}}{(p_{HCl})^3} \tag{8}$$

$$K_B = \frac{K_p'}{p_B^\circ} \tag{9}$$

$$\Sigma_N = \frac{p_N}{p_N^\circ} = \frac{K_N p_{NH_3}}{(p_{H_2})^{3/2}} \tag{10}$$

$$K_N = \frac{K_p''}{p_N^\circ} \tag{11}$$

and

$$\Sigma_B \Sigma_N = K \frac{p_{BCl_3} p_{NH_3}}{(p_{HCl})^3} \tag{12}$$

where $K = K_B K_N$. These relations are obviously also related to the degree of completion of the reactants conversion.

With regard to the CVD process and the structure of the deposits, high supersaturations and low temperatures are gen-

erally believed to lead to poor crystal organization.[34,35] Thus, it is not surprising that all the CVD deposits present a poor organization at 700°C (Fig. 8). Forced flow toward single fibers, thin tows, or 2D single cloth (either stationary or moving) can be used to obtain sufficiently uniform coatings that can be better organized at higher temperature.[36] The drawbacks of such a process, in terms of the amount of fibers that could be coated and processing complexity, are clear.

With regard to the ICVI process, the supersaturation is always lower than that with CVD at 700°C; however, the gas-phase chemistry also can be changed by the influence of different parameters. The residence time especially is greater, because of diffusion inside the preform; the conversion yield also is much higher, because of the specific surface of the porous preform. To first address the possible influence of the variation of the supersaturation, it is clear that some conditions lead to high supersaturations and then to poor organization of the ICVI deposits (for the experimental conditions that have been studied here, these conditions are classical ICVI with high flow rates and the external and upper positions in the preform). In contrast, all the deposits that have been elaborated via protected-ICVI exhibit greater coherent domains and smaller interlayer distances and dispersions, in comparison to similar coatings that have been obtained from the classical ICVI process. For both ICVI and protected-ICVI processes, an intermediate flow rate leads to the best organization of the film: in the case of protected-ICVI, the optimal organization is obtained for a higher mass flow rate than that for classical ICVI (see Figs. 9 and 12). This observation has been confirmed by the experiment that was conducted at a flow rate of 56×10^{-6} kg/s, which did not drastically debase the organization when protected-ICVI was used, in contrast to the experiment that was conducted without screens at a flow rate of 28×10^{-6} kg/s.

All these results show that the BN crystalline organization can be optimized under conditions where the ICVI process departs both from a pure mass-transfer control (i.e., from almost-total conversion at the gas/solid interface) and obviously from a pure kinetic control (which is obtained with CVD at high flow rates). These particular infiltration conditions are difficult to discuss, because this result might be attributed to different changes in the deposition mechanism. If the surface mechanism of the ICVI process remains unchanged from the limiting CVD process, the BN organization would be improved normally first at lower supersaturations. Although the poor organization of the ICVI deposits that have been obtained at high flow rates without protection is classical, deterioration of the structure at low flow rates is unusual. The poorest organization of the BN deposits has been obtained at the lowest flow rates, especially in downstream and inside locations (e.g., with a high deposition yield). This result might be attributed to a high HCl concentration, which could hamper the BN organization during growth, even if HCl does not act as an inhibitor for the heterogeneous reaction on the bulk substrates. On the other hand, the residence time of the gaseous species is changed through the infiltration itself, the variation of the total flow rate, and the use of diffusion screens. The homogeneous formation of intermediate precursors, which leads to a different surface mechanism that favors or hinders the organization of the BN deposit, cannot be excluded either. Evolution of the gas phase with time already has been observed in the deposition of pyrocarbon via pulsed CVD,[37] which is a process that allows the residence time to be monitored by using the pulse duration. The lattice organization and orientation is improved by intermediate "maturation times" of the gaseous phase, because particular intermediates could form. Therefore, other thorough studies would be necessary to understand how the BN organization is improved. The influence of the amount of HCl or the formation of intermediate species could especially be examined.

The above-mentioned discussion about the influence of the deposition conditions on the BN structure shows that the nature of the fiber obviously cannot influence the structure of the CVD deposits. In all cases, any possible influence on the initial growth conditions would be hidden by the unfavorable CVD conditions that have been used in this study. However, it seems that the structure can be improved by using a high-temperature post-treatment. In fact, only poorly organized films exhibit a skin effect in the outermost 10–20 nm of the BN coating. Although the graphitization of BN from a turbostratic structure only occurs at ~2000°C, it has been proved that the external reorganization was the result of the treatment at 1000°C under vacuum. Lacrambe[38] also has shown that moderate temperatures (1300°–1700°C) lead to better crystallization of BN that has been prepared via CVD. However, he attributed this improvement to the evolution of his samples when previously exposed to a moist environment. In our case, the substrates were kept in the reactor under vacuum between the deposition stage and the thermal post-treatment. However, they do contain oxygen as an impurity,[39] and they exhibit poor resistance to moisture when they are poorly organized.[30] It could then be suggested that the thermal treatment allows some decrease in the content of some impurities, such as oxygen and hydrogen atoms that are incorporated in the deposits. When they are removed, the BN lattice can rearrange. This phenomenon would be favored by an initially very poor organization, and it would be limited to the surface of the coatings. The structure of each of the BN sequences that are deposited by the alternate CVD process seems to be sufficiently organized to prevent such a reorganization. However, additional investigations are needed to valid these hypotheses.

V. Conclusions

From the results that have been presented in Section III and discussed in Section IV, the following conclusions can be drawn:

(1) The chemical vapor deposition (CVD) process is governed either by a combination of mass transfer with chemical kinetics at low flow rates or by the heterogeneous kinetics alone at higher flow rates. In this latter case, the deposition rate is dependent only on the lowest partial pressure of the reactants (BCl_3 or NH_3), and a very good longitudinal uniformity of the deposit thickness is obtained. At a deposition temperature of 700°C, the supersaturation is high in any case. For the isothermal–isobaric chemical vapor infiltration (ICVI) process, the limiting contribution of mass transfer is always observed, because of diffusion of the gaseous phase in the fibrous substrate and the great deposition yield (because of its high specific surface area). Therefore, the influence of the concentration of the inlet reactant species on the deposition rate is more complex. The deposition rate is lower than that observed in the CVD process, and, accordingly, the supersaturation is much lower.

(2) The structure of BN coatings that have been deposited from BCl_3–NH_3–H_2 mixtures is highly dependent on the deposition conditions, including the processing type (CVD or ICVI, protected or not by diffusion screens). The present CVD conditions lead to poor organization of the BN deposits with a large interlayer spacing, in accordance to the high supersaturation. The ICVI process allows deposition of a fairly well-organized BN coating on all fibers of a fibrous preform under conditions where the supersaturation is intermediate. Poorer organization that is obtained at lower supersaturation could be due to the high yield of deposition, which leads to important HCl formation and very different deposition conditions at the gas/solid interface. The influence of the formation of intermediate species that are produced by some homogeneous reactions cannot be excluded under conditions where the residence time also is very different. However, additional studies are necessary to validate these hypotheses.

(3) Good thickness uniformities can be obtained via ICVI, despite the influence of mass transfer. In regard to that point, the gaseous product HCl has no influence on the deposition rate. The use of diffusion screens and the adjustment of the

inlet composition and the mass flow rate seem to be very important to obtain both the best uniformity and the best organization. The use of diffusion screens especially could be generalized to other systems, to improve the control of the deposit structure.

(4) A thermal post-treatment at 1000°C under vacuum improves the organization of BN that has been deposited via CVD only. However, the reorganization is limited to the outermost 10–20 nm of the layer, and it seems to require an initially very poor organization and the release of impurities.

Acknowledgments: The authors acknowledge R. Herbin, for her help in the preparation of the samples and the manuscript, and Y. Boussant, for his technical contribution. The authors also are indebted to S. Goujard and C. Robin-Brosse (SEP) for the supply of materials and fruitful discussions.

References

[1]J. Aveston, G. Cooper, and A. Kelly, "Single and Multiple Fracture"; pp. 15–26 in *Properties of Fibre Composites*, Proceedings of the Conference of the National Physics Laboratory. IPC Science Technology Press, Ltd., Guildford, England, 1971.

[2]J. W. Hutchinson and H. Jensen, "Models of Fiber Debonding and Pull-out in Brittle Composites with Friction," *Mech. Mater.*, **9**, 139–63 (1990).

[3]A. G. Evans and D. B. Marshall, "The Mechanical Behavior of Ceramic Matrix Composites," *Acta Metall.*, **37**, 2567–83 (1989).

[4]R. W. Davidge, "Fibre-Reinforced Ceramics," *Composites (Guildford UK)*, **18**, 92–98 (1987).

[5]J. J. Brennan, "Interfacial Chemistry and Bonding in Fiber-Reinforced Glass and Glass-Ceramic Matrix Composites," *Mater. Sci. Res.*, **21**, 387–99 (1986).

[6]R. F. Cooper and K. Chyung, "Structure and Chemistry of Fibre-Matrix Interfaces in Silicon Carbide Fibre-Reinforced Glass-Ceramic Composites: An Electron Microscopy Study," *J. Mater. Sci.*, **22**, 3148–60 (1987).

[7]J. M. Jouin, J. Cotteret, and F. Christin, "SiC–SiC Interphases: Case History"; pp. 191–204 in *Proceedings of the 2nd European Colloquium (Designing Ceramic Interfaces)* (Nov. 11–13, 1991, Petten, The Netherlands). Edited by S. D. Peteves. CEC, Petten, The Netherlands, 1993.

[8]R. Naslain, "Fibre–Matrix Interphases and Interfaces in Ceramic Matrix Composites Processed by CVI," *Compos. Interfaces*, **1**, 253–86 (1993).

[9]C. Vix-Guterl, J. Lahaye, and P. Ehrburger, "Reactivity in Oxygen of a Thermostructural Composite"; pp. 725–32 in *High Temperature Ceramic Matrix Composites.* Edited by R. Naslain, J. Lamon, and D. Doumeingts. Woodhead Publishing Limited, Abington, Cambridge, England, 1993.

[10]D. H. Grande, "Fibre–Matrix Bond Strength Studies of Glass, Ceramic, and Metal Matrix Composites," *J. Mater. Sci.*, **23**, 311–28 (1988).

[11]M. P. Bacos, "Carbon–Carbon Composites: Oxidation Behavior and Coatings Protection," *J. Phys. IV*, **3**, 1895–903 (1993).

[12]S. Goujard, L. Vandenbulcke, and H. Tawil, "Oxidation Behavior of 2D and 3D Carbon/Carbon Thermostructural Materials Protected by CVD Polylayer Coatings," *Thin Solid Films*, **252**, 120–30 (1994).

[13]A. W. More, M. B. Dowell, E. R. Stover, and L. D. Bentsen, "Oxidation Protection of Carbon–Carbon Composites by (B+Si)N Coatings," *Ceram. Eng. Sci. Proc.*, **16**, 263–70 (1995).

[14]R. J. Diefendorf and R. R. Boisvert, "Processing of Polymeric Precursor Ceramic Matrix Composites," *Mater. Res. Soc. Symp. Proc.*, **120**, 157–62 (1988).

[15]L. Héraud, R. Naslain, and J. M. Quenisset, "Procédé de Fabrication d'un Matériau Composite à Matrice Céramique à Ténacité Améliorée," Fr. Pat. No. 89.02718, March 2, 1989.

[16](a) C. Droillard, "Elaboration et Caractérisation de Composites à Matrice SiC et à Interphase Séquencée C/SiC"; Ph.D. Thesis No. 913. Bordeaux University, Talence, France, 1993. (b) C. Droillard, J. Lamon, and X. Bourrat, "Strong Interface Bonding in CMCs, Conditions for Efficient Multilayered Interphases," *Mater. Res. Soc. Symp. Proc.*, **365**, 371–76 (1995).

[17]L. Vandenbulcke and S. Goujard, "Multilayer Systems Based on B, B_4C, SiC and SiBC for Environmental Composite Protection"; pp. 1198–204 in *Progress in Advanced Materials and Mechanics.* Edited by T. Wang and T.-W. Chou. Peking University Press, Beijing, China, 1996.

[18]R. A. Lowden, K. L. More, O. J. Schwarz, and N. L. Vaughn, "Improved Fiber–Matrix Interlayers for Nicalon/SiC Composites"; see Ref. 9, pp. 345–52.

[19]J. M. Agullo, F. Maury, and J. M. Jouin, "Mechanical Properties of SiC/SiC Composites with a Treatment of the Fiber/Matrix Interfaces by Metal-organic Chemical Vapor Co-deposition of C and Si_xC_{1-x}," *J. Phys. IV*, **3**, 549–56 (1993).

[20]T. Matsuda, "Stability to Moisture for Chemically Vapour-Deposited Boron Nitride," *J. Mater. Sci.*, **24**, 2353–58 (1989).

[21]K. P. Norton and H. H. Streckert, "Effect of BN Interfacial Coating on the Strength of a Silicon Carbide/Silicon Nitride Composite," *Mater. Res. Soc. Symp. Proc.*, **250**, 239–44 (1992).

[22]M. A. Kmetz, J. M. Laliberte, W. S. Willis, and S. L. Suib, "Synthesis, Characterization, and Tensile Strength of CVI SiC/BN/SiC Composites," *Ceram. Eng. Sci. Proc.*, **12**, 2161–74 (1991).

[23]R. Naslain, O. Dugne, A. Guette, J. Sevely, C. Robin Brosse, J.-P. Rocher, and J. Cotteret, "Boron Nitride Interphase in Ceramic-Matrix Composites," *J. Am. Ceram. Soc.*, **74** [10] 2482–88 (1991).

[24]N. Ricca, A. Guette, G. Camus, and J. M. Jouin, "SiC (ex-PCS) MAS Composites with a BN Interphase: Microstructure, Mechanical Properties and Oxidation Resistance"; see Ref. 9, pp. 455–62.

[25]S. Prouhet, G. Camus, C. Labrugère, A. Guette, and E. Martin, "Mechanical Characterization of Si-C(O) Fiber/SiC (CVI) Matrix Composites with a BN-Interphase," *J. Am. Ceram. Soc.*, **77** [3] 649–56 (1994).

[26]E. Y. Sun, S. R. Nutt, and J. J. Brennan, "Interfacial Microstructure and Chemistry of SiC/BN Dual-Coated Nicalon-Fiber-Reinforced Glass-Ceramic Matrix Composites," *J. Am. Ceram. Soc.*, **77** [5] 1329–39 (1994).

[27]O. Dugne, S. Prouhet, A. Guette, R. Naslain, R. Fourmeaux, Y. Khin, J. Sevely, J.-P. Rocher, and J. Cotteret, "Interface Characterization by TEM, AES, and SIMS in Tough SiC (ex-PCS) Fibre–SiC (CVI) Matrix Composites with a BN Interphase," *J. Mater. Sci.*, **28**, 3409–22 (1993).

[28]J. J. Brennan, "Interfacial Studies of Chemical-Vapor-Infiltrated Ceramic Matrix Composites," *Mater. Sci. Eng. A*, **A126**, 203–23 (1990).

[29]B. A. Bender and T. L. Jessen, "A Comparison of the Interphase Development and Mechanical Properties of Nicalon and Tyranno SiC Fiber-Reinforced $ZrTiO_4$ Matrix Composites," *J. Mater. Res.*, **9**, 2670–76 (1994).

[30]M. Leparoux, "Elaboration à Partir de la Phase Gazeuse des Interphases BN et BNSi pour Composites SiC/BN(Si)/SiC, Structure et Propriétés des Matériaux Obtenus"; Ph.D. Thesis. Université d'Orléans, Orleans, France, 1995.

[31]M. Leparoux and L. Vandenbulcke, "Influence of the CVD and ICVI Processes on the Boron Nitride Deposition Kinetics"; pp. 594–98 in *Proceedings of the 13th International Conference on Chemical Vapor Deposition*, Electrochemical Society Proceedings, Vol. 96-5. Edited by T. M. Besmann, M. D. Allendorf, McD. Robinson, and R. K. Ulrich. Electrochemical Society, Pennington, NJ, 1996.

[32]V. Cholet and L. Vandenbulcke, "Chemical Vapor Infiltration of Boron Nitride Interphase in Ceramic Fiber Preforms: Discussion of Some Aspects of the Fundamentals of the Isothermal Chemical Vapor Infiltration Process," *J. Am. Ceram. Soc.*, **76** [11] 2846–58 (1993).

[33]N. Patibandla and K. L. Luthra, "Chemical Vapor Deposition of Boron Nitride," *J. Electrochem. Soc.*, **139**, 3558–65 (1992).

[34]L. Vandenbulcke and G. Vuillard, "Structure of Deposits–Process Relationships in the Chemical Vapor Deposition of Boron," *J. Electrochem. Soc.*, **124**, 1937–42 (1977).

[35]J. M. Blocher Jr., "Structure/Property/Process Relations in Chemical Vapor Deposition CVD," *J. Vac. Sci. Technol.* **11**, 680–86 (1974).

[36]B. L. Weaver, R. A. Lowden, J. C. McLaughlin, D. P. Stinton, T. M. Besmann, and O. J. Schwarz, "Nextel/SiC Composites Fabricated Using Forced Chemical Vapor Infiltration"; see Ref. 9, pp. 353–60.

[37]P. Dupel, R. Pailler, and X. Bourrat, "Pulse-CVD and Infiltration of Pyrocarbon in Model Pores with Rectangular Cross-Sections: Part II, Study of the Infiltration," *J. Mater. Sci.*, **29**, 1056–66 (1994).

[38]G. Lacrambe, "Fabrication et 'Graphitation' du Nitrure de Bore Obtenu par Dépôt Chimique en Phase Vapeur à Basse Température"; Ph.D. Thesis No. 2232. Bordeaux University, Talence, France, 1988.

[39]M. Leparoux, L. Vandenbulcke, V. Serin, and J. Sevely, "The Interphase and Interface Microstructure and Chemistry of Isothermal/Isobaric Chemical Vapour Infiltration SiC/BN/SiC Composites: TEM and Electron Energy Loss Studies," *J. Mater. Sci.*, **32**, 4595–602 (1997). □